Polymer 55 (2014) 5017–5023

Contents lists available at ScienceDirect

Polymer

journal homepage: www.elsevier.com/locate/polymer

Polymer communication

High definition fibrous poly(2-ethyl-2-oxazoline) scaffolds through melt electrospinning writing

Gernot Hochleitner [a, 1], Julia Franziska Hümmer [a, 1], Robert Luxenhofer [b], Jürgen Groll [a, *]

[a] Department for Functional Materials in Medicine and Dentistry, University of Würzburg, Pleicherwall 2, 97070 Würzburg, Germany
[b] Functional Polymer Materials, Chair of Chemical Technology of Materials Synthesis, University of Würzburg, Röntgenring 11, 97070 Würzburg, Germany

ARTICLE INFO

Article history:
Received 6 May 2014
Received in revised form
4 August 2014
Accepted 12 August 2014
Available online 27 August 2014

Keywords:
Polymer processing
Poly(2-oxazoline)
High temperature melt electrospinning writing

ABSTRACT

Melt electrospinning writing (MEW), a computer-aided fiber deposition process based on an electrohydrodynamic working principle, enables the rational design and fabrication of fibrous scaffolds with micrometer thin fibers. So far, MEW has mainly been applied for poly(ε-caprolactone). Here we manufactured scaffolds of poly(2-ethyl-2-oxazoline), a hydrophilic polymer with high melting temperature, by MEW for the first time. We systematically varied and investigated the crucial instrument parameters: heating temperature (200–220 °C), feeding pressure (1.0–3.0 bar), accelerating voltage (3.0–7.0 kV) and collector distance (3.0–7.0 mm) in dependence of differently sized spinnerets (23 G, 25 G, 27 G, 30 G). As criteria for homogeneous deposition, we studied the resulting fiber diameters which could be adjusted from 8 μm to 138 μm and the corresponding variances. Furthermore this letter clarifies the need of a dynamic balance between involved mass flows in order to reduce pulsing failures of the jet and thereby structural defects of the deposited structures.

1. Introduction

Research into the class of hydrophilic polymers, called poly(2-oxazoline)s (POx) has intensified over the past decade [1–7]. Synthesized via living cationic ring-opening polymerization [3], the macromolecular structure of POx is readily adjustable to produce a versatile spectrum of properties with potential for medical and pharmaceutical applications. POx is particularly interesting as a drug delivery system and is thermoresponsive with a characteristic lower critical solution temperature [8,9].POx-based polymers can have stealth-properties similar to poly(ethylene glycol), are biologically compatible and can store pharmaceutical agents, including functional proteins mimicking natural biomolecules or act as antimicrobial materials [10–12]. While the chemical and physical properties of POx are appreciated, how to process the polymer into discrete structures is still being understood. Owing to its thermoplastic and electrically non-conductive properties, POx offers the potential to be processed via melt electrospinning. When combined with a translating collector, there is also potential to 3D print POx using additive manufacturing principles, potentially allowing infinite different structures to be generated with this polymer.

Another biocompatible polymer poly(ε-caprolactone) (PCL) has already been processed into 3D printed scaffolds using this direct writing technique, termed melt electrospinning writing (MEW) [13–15]. With fiber deposition assisted by a computer-controlled axis movement of the collector, it allows the 3D stacking of fibrous structures filaments as low as 5 μm in diameter. This progress is so far focused specifically for biomedical research and TE applications [15,16]. Electrospinning is based on an electrohydrodynamic working principle, investigated heavily over the past decade [17–19]. Nevertheless, the stable electrified molten jet is not extensively investigated compared to its analogue – solution electrospinning [20]. In both cases the applied acceleration voltage reaches a critical value and thereby overcomes the surface tension of a fluid. A Taylor cone forms and an electrified polymer jet is accelerated by the electrical field to the collector system. Influencing parameters are classified as polymer-based (e.g. molar mass) and instrument based (e.g. voltage, collection distance etc.).

We show in this study, that one type of POx, poly(2-ethyl-2-oxazoline (PEtOx)), can not only be successfully melt electrospun, it is an excellent polymer for performing MEW. Several key instrument parameters to attain a stable molten jet were systematically investigated, including heating temperature, feeding

* Corresponding author. Tel.: +49 931 20173610; fax: +49 931 20173500.
E-mail address: juergen.groll@fmz.uni-wuerzburg.de (J. Groll).
[1] Tel.: +49 931 20173610; fax: +49 931 20173500.

http://dx.doi.org/10.1016/j.polymer.2014.08.024

pressure, accelerating voltage, the collector distance and spinneret diameter. Through adjustment of the parameters, quality woodpile structures of PEtOx could be produced by MEW.

2. Experimental methods

2.1. Materials

Poly(2-ethyl-2-oxazoline) (PEtOx) with $M_w \approx 50{,}000$ g/mol and PDI ≈ 3–4 was purchased from Sigma–Aldrich (372846) and used as received.

2.2. Melt electrospinning writing device

The MEW device, schematically drawn in Fig. 1, consists of a high voltage source (DX250R, EMCO, Hallein, Austria) controlled by voltage divided measurement (Digit Multimeter 2100, Keithley, Cleveland, USA), a nitrogen gas pressured assisted melt feeding system (regulator, FESTO, Berkheim, Germany) and a planar movable aluminum collector plate (XSlide, Velmex, New York, USA), triggered by G-code (MACH 3 CNC software, ARTSOFT, Livermore Falls, USA). To assure a stable heating temperature profile a proportional-integral-derivative-regulated (TR400, Delta-t, Bielefeld, Germany) electrical heating system was used.

2.3. Parameter range

Key instrument parameters were varied in five consistent steps with four different spinnerets (30 G: $d_I = 160$ μm, 27 G: $d_I = 210$ μm, 25 G: $d_I = 260$ μm, 23 G: $d_I = 337$ μm). Only a parameter was changed at a time, with the other parameters kept constant at the middle value of the parameter range, shown in Table 1. The collector velocity was adjusted (between 200 mm min^{-1} and 400 mm min^{-1}) to be just above the critical translation speed, which is the transition point between coiled and straight fibers. This ensures a straight fiber with diameters that are not stretched by the movement of the collector. To characterize the statistical significance, respectively probability p of the results, every set of parameters was investigated by the measurement of $n = 20$ fiber diameters and evaluated by analysis of variance (ANOVA).

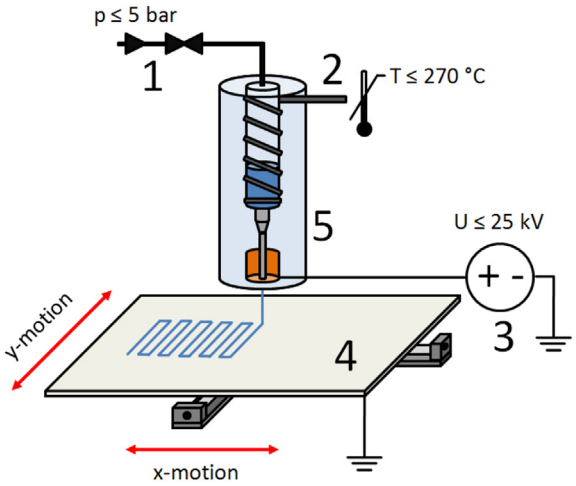

Fig. 1. Schematic drawing of the MEW device. 1) Nitrogen gas pressure assisted feeding system 2) Electrical heating system 3) High voltage source 4) Computer assisted movable collector plate 5) Syringe with molten polymer and needle tip as spinneret with electrode.

Table 1
Overview of the investigated instrument parameters.

Parameter	Parameter range	Constant value
Temperature T_h [°C]	200 to 220	210
Feeding pressure p_f [bar]	1.0 to 3.0	2.0
Acceleration voltage U_a [kV]	3.0 to 7.0	5.0
Collector distance L_c [mm]	3.0 to 7.0	5.0
Spinneret [Gauge]	23, 25, 27, 30	N/A[a]

[a] All four other instrument parameters were tested with the different spinnerets.

2.4. Scanning electron microscopy

Field emission scanning electron microscopy (SEM) images were recorded (Ultra Plus, Carl Zeiss AG, Oberkochen, Germany) using a GEMINI e-Beam column operated at 1–3 kV with an aperture size set to 10 μm to avoid excessive charging and radiation damage of the areas imaged. Gold deposition onto the samples was performed by sputtering technique using a cryo-preparation system Quorum PP2000 for 2 min at emission of 20 mA. The argon pressure in the chamber was set to $8 \bullet 10^{-2}$ mbar.

3. Results and discussion

The main focus of this work was instrument parameter combinations to optimize the fiber variability and quality and understand how best to control the fiber diameter of PEtOx. A key challenge was “pulsing” of the electrified molten jet, where fibers alternated between thick and thin, resulting in poor quality collections. As a result, many parameter combinations did not lead to desired fiber accuracies, with photographs of the defects shown in Fig. 2.

The greatest variations in fiber diameter occurred when the 23 G spinneret was used, suggesting that this spinneret diameter is too large for the polymer and conditions. Fig. 3 gives an overview on the studied parameters. It shows the relationship between fiber diameter and temperature – when the temperature is increased from 200 to 220 °C, the diameter of the deposited fibers increased significantly ($p < 0.01$) with an average value of 45 μm raising to 138 μm for the 23 G spinneret. The challenges faced with fluctuating fiber diameter are well reflected in the large error bars for the data presented in Fig. 3. The fibers were generally more homogeneous fibers at lower temperatures and pressures, as well as with higher acceleration voltages due to the approximation of the involved mass flows.

Considering that the pulsing effect was particularly significant for the largest (23 G) spinneret investigated, we looked at the mass flow of the melt, based on a dynamic balancing process. That is, the push of the melt to the spinneret versus the pull of the melt due to electrostatic attraction. Relevant here is the Hagen-Poiseuille-equation [21,22], which shows the dominating dependency of flow rates dm/dt from the spinneret diameter d_o with:

$$\frac{dm}{dt}\left[1\right] \sim d_o^4$$

Therefore, the mass flows and deposited fibers should be even smaller with smaller spinneret diameters and proper mass flow adjustment. Due to an almost constant average jet velocity (200 mm min^{-1}) and a circular fiber profile, an increase of the gas pressure assisted mass flow dm/dt by one order of magnitude could be obtained using the 23 G spinneret. This can be explained by the lowered loss and storage modulus of the melt during heating from 200 to 220 °C and seems to be more influencing as the triplication of the feeding pressure at 210 °C. Accordingly, the minimal average diameter was 58 μm at 1.0 bar and 118 μm at 3.0 bar. Thus, the mass

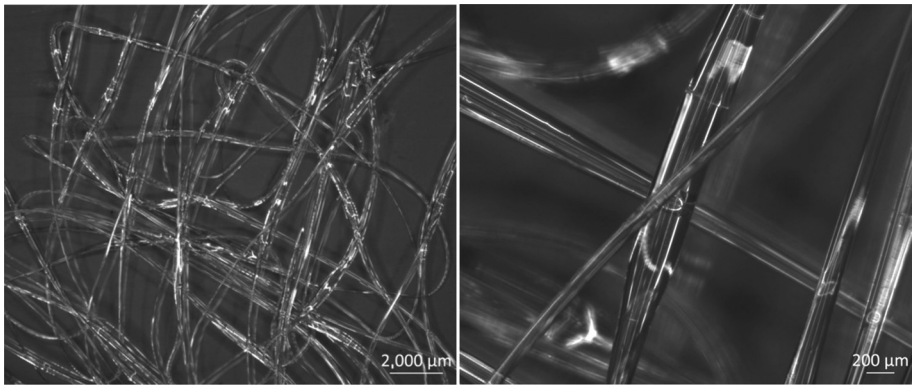

Fig. 2. Deposited PEtOx fibers show two types of appeared electrospinning failures. The pulsing failure led to a broad variance of fiber diameters, while inhomogeneous charge repulsion effects prohibited a well-defined deposition. Following instrument parameters were applied: T_h = 210 °C, p_f = 3.0 bar, U_a = 5.0 kV, L_c = 5.0 mm, spinneret: 23 G, v_{col} = 200 mm min^{-1}.

flow dm/dt increased approximately four times ($p < 0.01$). In addition the variance increased significantly, which can be explained by consideration of the dynamic balance of the average mass flows (Fig. 4) referring to the law of conservation of mass with: $d\overline{m}/dt$ [1] = dm/dt [1] = constant equates to $d\overline{m}/dt$ [2]. In this context, $d\overline{m}/dt$ [2] is the sum of the average electrohydrodynamic and average mechanical drawing dominated mass flows: $d\overline{m}/dt$ [E], respectively $d\overline{m}$ /dt [M].

If the constant mass flow $d\overline{m}/dt$ [1], induced by the gas pressure assisted feeder, exceeds the mass flow induced by the electrohydrodynamic drawing dm/dt [E] of the jet, the variance of the deposited fibers increases apparently. This is, amongst others, caused by a melt mass accumulation at the spinneret and an intermittent delay in mass output. If this mass accumulation is increasing, mechanical jet stretching effects and subsidiary gravity gain more relative influence on the jet-related mass flow compared to the predominant electrical field. This phenomenon results in a dynamic swaying of physical momentum, force balance and thus mass flows. These unadjusted mass flows led to a change in jet velocity during the electrospinning process and at a certain difference between jet and collector velocity – the mechanical drawing became predominant. As a result temporally varying dm/dt [2] appears. In contrast to common melt electrospinning methods such mechanical couplings play a significant role in means of fiber diameter and homogeneity of the deposition process. This effect can be described as pulsing failure and is a complex

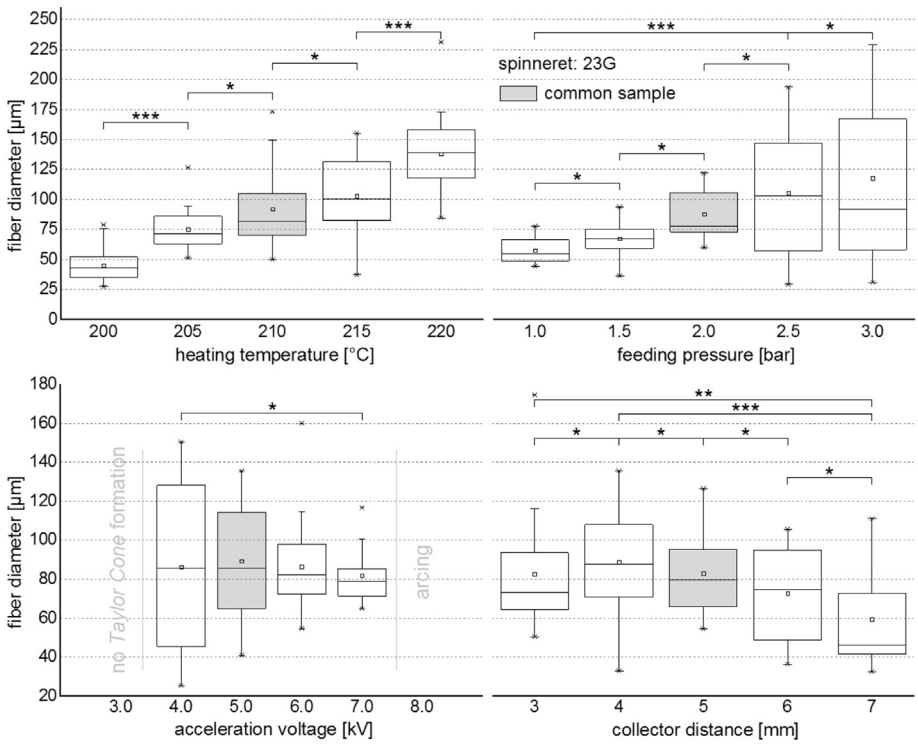

Fig. 3. Deposited fiber diameter as a function of heating temperature, feeding pressure, acceleration voltage and collector distance using a 23 G spinnerets. The fiber diameter was increasing linearly with increasing temperature and feeding pressure. Further, the variance of the deposited fibers was increasing significantly with increasing pressure and decreasing acceleration voltage. While the collector distance increased, the acceleration voltage stayed constant. Hence, the electrical field strength decreased. * non-significant/** $p < 0.05$/*** $p < 0.01$.

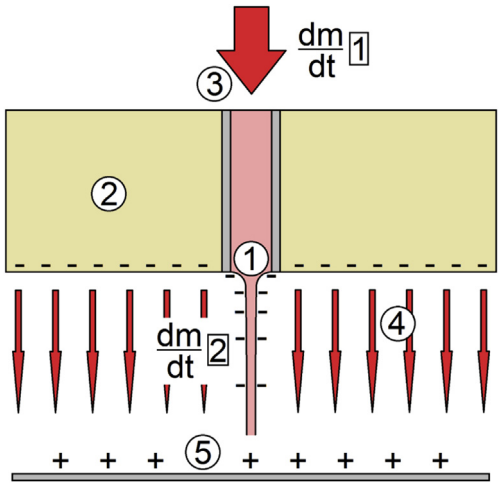

Fig. 4. Schematic drawing of the MEW mass flows. The gas pressure assisted feeding system induces mass flow dm/dt [1] as a function of the pressure, feeder geometry and the viscoelastic properties of the polymer melt. Mass flow dm/dt [2] is determined by the surface charge density, set-up geometry, acceleration voltage and the viscoelastic properties of the solidifying jet. 1) Polymer melt and Taylor Cone, 2) High voltage electrode, 3) Gas pressure assisted feeding, 4) Electrical field, 5) Collector plate.

interaction between participating factors like the viscoelastic properties, set-up geometry, feeding pressure, charge density of the jet surface and acceleration voltage.

This pulsing phenomenon was also observed while studying the influence of the acceleration voltage on the fiber diameter. At 8.0 kV and higher voltages, arcing occurred, whereas 3.0 kV and lower voltages did not lead to a Taylor Cone formation. While no significant change in diameter appeared, because dm/dt [1] stayed constant during these series, the variance decreased strongly with increasing voltage. This observation hypothesizes a decrease of dynamic swaying amplitude while the acceleration voltage was increasing, caused by a lowered difference between $d\overline{m}/dt$ [1] and dm/dt [E]-induced jet stretching. This realization clarifies the necessity of an adjusted parameter process.

In contrast to the other factors, an increase in collector distance for the 23 G spinneret slightly decreased the fiber diameter from 83 μm at 3.0 mm to 60 μm at 7.0 mm with a constant acceleration voltage ($p < 0.05$). In this context the decrease of electrical field strength – a constant acceleration voltage divided by an increasing collector distance – must be considered. In theory this increasing field strength should lead to lesser electrical stretching forces and therefore thicker and slower jets. But with increasing collector distance the acceleration path also increases, which allows a further time-dependent stretching of the viscoelastic polymer jet. This increased acceleration distance predominated the decreased electrical field strength and led to smaller fiber diameters.

Summarizing the parameter study at constant spinneret size of 23 G, the most important influence was determined by increasing the temperature at constant pressure, acceleration voltage and collector distance. This implies the dominating influence of the viscoelastic polymer properties which are connected to the heating temperature.

As already described in literature [23,24], the size of the spinneret has a significant influence on the deposited fiber diameter. When looking at the Hagen-Poiseuille-equation, the smaller diameters should also have less “pulsing”, and this is what we observed. As shown in Fig. 5 the diameters of the fibers produced with 25 G, 27 G and 30 G spinnerets were smaller and had less of a distribution compared to those processed by a 23 G spinneret.

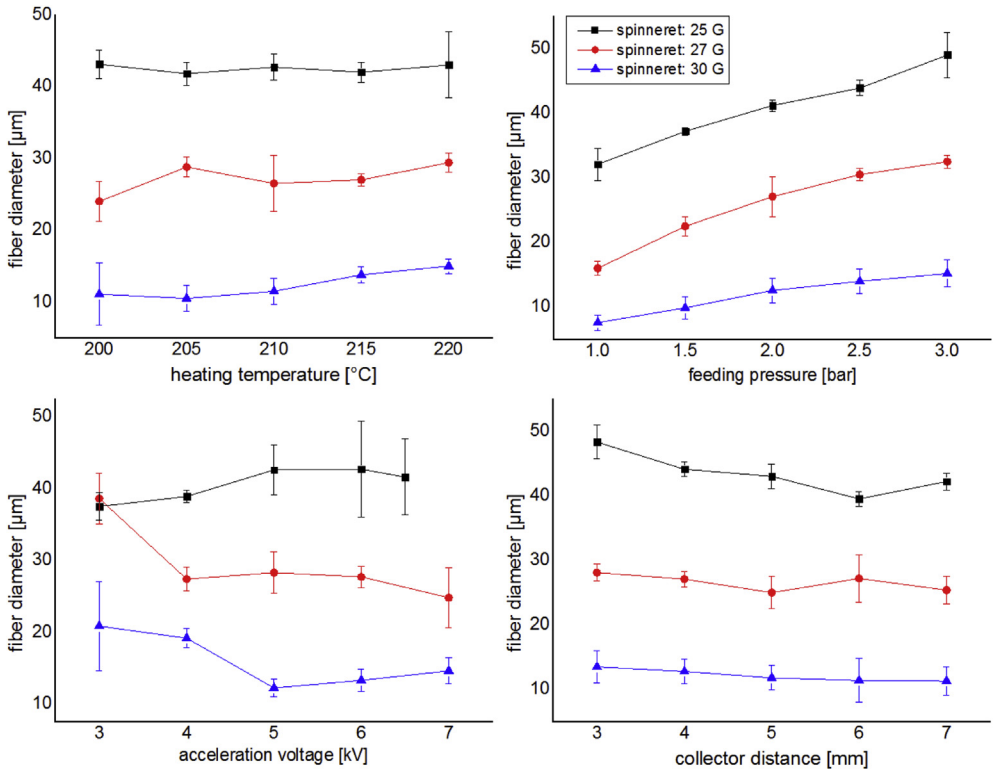

Fig. 5. Deposited fiber diameter as a function heating temperature, feeding pressure, acceleration voltage and collector distance using 25 G, 27 G and 30 G spinnerets. With increasing spinneret diameter, heating temperature and feeding pressure the deposited fiber diameter increased. With increasing collector distance the fiber diameter decreased slightly.

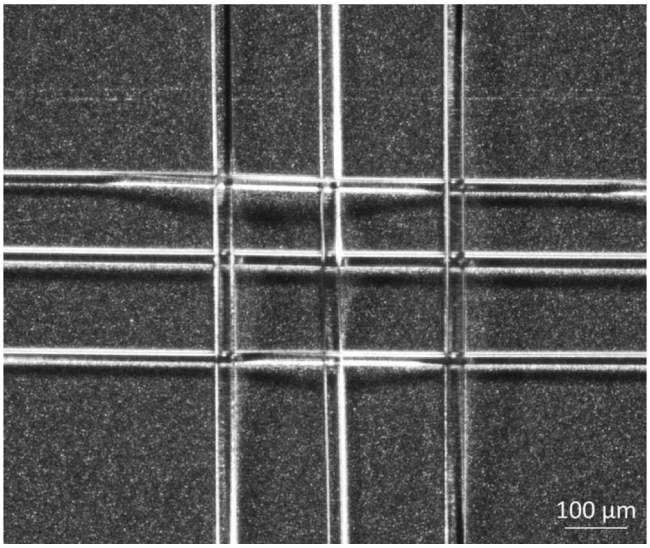

Fig. 6. Homogeneous deposited fibrous PEtOx structures fabricated via MEW. Following instrument parameters were applied: T_h = 210 °C, p_f = 1.5 bar, U_a = 3.0 kV, L_c = 4.0 mm, spinneret: 27 G, v_{col} = 400 mm min^{-1}.

Nevertheless, the adjustment of mass flows is very important in order to fabricate homogeneous fibers. While significant "pulsing" failures occurred by using a 23 G spinneret with 220 °C or 3.0 bar, these instrument parameters did not lead to "pulsing" of the 30 G electrospun jets. This is caused by smaller fed mass flows dm/dt [1] of the smaller spinneret diameter and thereby proper adjusted process balancing (dm/dt [1] ≈ dm/dt [E]). This argumentation is consistent to the obtained diameters and their corresponding deviations processed by 25 G and 27 G spinnerets, which lay in between the fiber diameters fabricated with 23 G and 30 G.

Regarding the influence of the feeding pressure on the fiber diameter in a linear way, as long as the mass flow adjustment was given for the series of tests (25 G, 27 G, 30 G), the equation of Hagen-Poiseuille was confirmed in our study. This could be shown by the comparison of the feeding pressure with 1.0–3.0 bar and the resulting approximate triplication or quadruplicating of average fiber cross-section area (23 G: 58 ± 10 µm to 118 ± 83 µm; 25 G: 32 ± 3 µm to 49 ± 4 µm; 27 G: 16 ± 1 µm to 33 ± 1 µm and 30 G: 8 ± 1 µm to 15 ± 2 µm) with constant collector respectively jet velocities due to:

$$\frac{dm}{dt}[1] \sim p$$

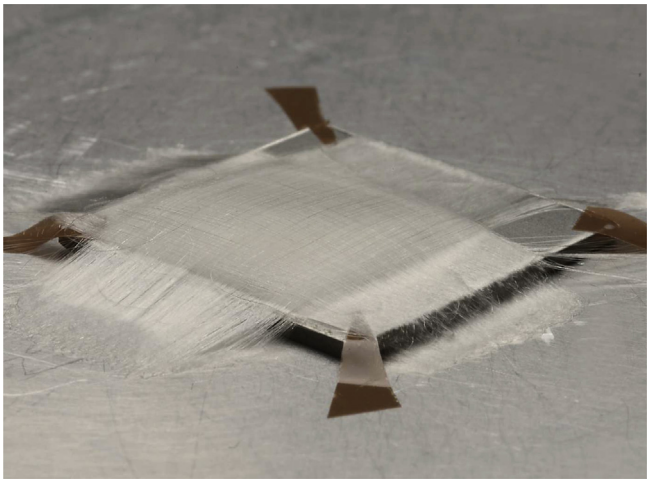

Fig. 8. Scaffold composed of PEtOx fabricated by MEW with 180 layers. Following instrument parameters were applied: T_h = 210 °C, p_f = 2.0 bar, U_a = 4.0 kV, L_c = 5.0 mm, spinneret: 30 G, v_{col} = 400 mm min^{-1}.

This implies that no significant extensional flow could have occurred due to flow velocity induced elongation of the macromolecules in the capillary or a thermally induced relaxation process could have been compensated the aligning effect of the molten polymer flow. Smaller sized diameters and relative deviations could be electrospun with smaller spinnerets, even at higher temperatures.

In contrast to the resulting fiber diameter processed with the 23 G spinneret, the acceleration voltage played no significant or negligible role in view of the deposited fiber diameters with 25 G, 27 G and 30 G spinnerets. In most cases the fiber cross-section became thinner, but a clear observation was not possible due to the dominating variance of the process. This could be the result of inhomogeneous electrically behavior of the PEtOx to the increasing acceleration voltage.

With increasing collector distance (3.0–7.0 mm) and thereby decreasing electrical field strength (1 $^2/_3$ to $^5/_7$ kV mm^{-1}) the fiber diameter is decreasing slightly with a 23 G spinneret: 83 ± 28 µm to 60 ± 27 µm; 25 G: 48 ± 3 µm to 42 ± 1 µm; 27 G: 28 ± 1 µm to 25 ± 2 µm and 30 G: 14 ± 2 µm to 11 ± 1 µm. This can be explained by the elongation of the collector distance as path for the acceleration as a stretching and thinning acting process.

This systematical investigation led to electrospinning of well-designed PEtOx scaffolds. As shown in Fig. 6 and Fig. 7, adjusted instrument parameters (T_h = 210 °C, p_f = 1.5 bar, U_a = 3.0 kV,

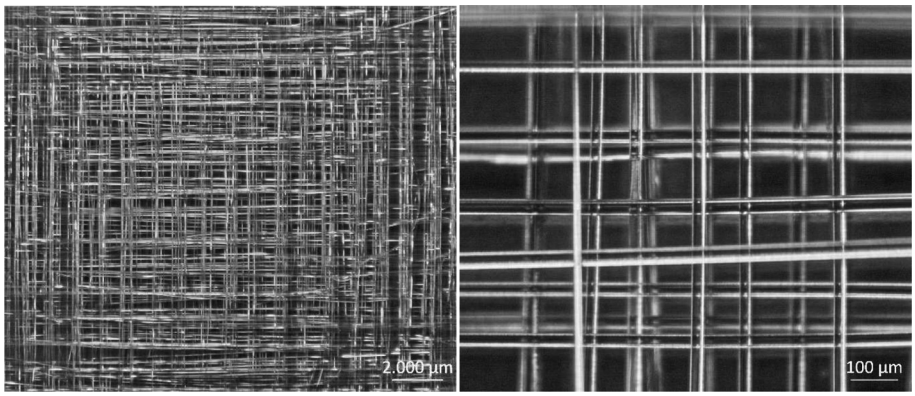

Fig. 7. Scaffold composed of PEtOx fabricated by MEW with 30 layers. Following instrument parameters were applied: T_h = 210 °C, p_f = 2.0 bar, U_a = 4.0 kV, L_c = 5.0 mm, spinneret: 27 G, v_{col} = 400 mm min^{-1}.

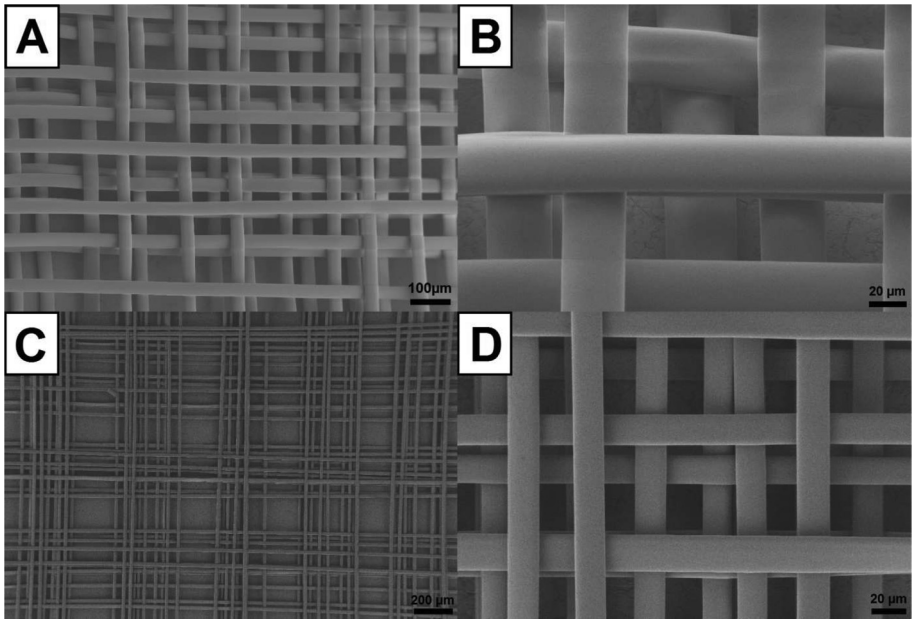

Fig. 9. SEM pictures of homogeneous deposited fibrous PEtOx structures fabricated via MEW. Following instrument parameters were applied: $T_h = 210$ °C, $p_f = 2.0$ bar, $U_a = 4.0$ kV, $L_c = 5.0$ mm, spinneret for A and B: 27 G, spinneret for C and D: 30 G, $v_{col} = 400$ mm min^{-1}.

$L_c = 4.0$ mm, spinneret: 30 G, $v_{col} = 400$ mm min^{-1}, respectively $p_f = 2.0$ bar, $U_a = 4.0$ kV, $L_c = 5.0$ mm) result in advanced process control and defined fiber macrostructures. To obtain 3D scaffolds with different homogeneous fiber diameters, additional parameter combinations ($T_h = 210$ °C, $p_f = 2.0$ bar, $U_a = 4.0$ kV, $L_c = 5.0$ mm, spinneret: 30 G, $v_{col} = 400$ mm min^{-1}) were ascertained. The diameters for all the investigated instrument parameters fibers ranged from 8 to 138 µm.

For these experiments to be considered an exercise in 3D printing, it is important to stack fibers upon each other. Due to residual electrostatic charges after deposition, and shielding effects, this is not always to be expected. We found that while some failures in the accurate fiber stacking were observed, we were able to manufacture organized, well-defined, scaffolds with more than 2 mm height (Fig. 8) under certain parameters. Overall, while there were some defects in fiber diameter and stacking, the PEtOx investigated was well processed using MEW and could be stacked into significant heights. However to attain small variations in fiber diameter and observe specific trends in instrument parameters such as flow rate, it is key that the diameter of the spinneret is small enough to balance the Hagen-Poiseuille-equation with the electrohydrodynamic induced mass flow of the jet, as shown in Fig. 9.

This study will serve as solid basis for the generation of hydrophilic and thermoresponsive scaffolds with immense potential for tissue engineering. A particular advantage here is the sharp transition temperature for POx that can be adjusted through polymer synthesis in the physiological temperature range to allow switching to water solubility at temperatures that do not negatively affect cell viability. This will for example allow releasing embedded bioactive compounds on demand through temperature changes. Moreover, such scaffolds will be extremely useful as sacrificial structural components within three dimensional hydrogels to generate vascular or neural structures.

4. Conclusion

Fibrous 3D scaffolds of PEtOx were processed in a broad range of diameters (8–138 µm) via MEW, which offers the potential to manufacture different structured scaffolds or components for TE. We systematically investigated key instrument parameters: heating temperature, feeding pressure, acceleration voltage and collector distance combined with different sized spinnerets. The resulting deposited fiber diameters and corresponding variances provided information about feasibility, instrument parameter interactions and limitations of this technique under investigated conditions. In this context, an increase in feeding pressure and temperature increased the deposited fiber diameters significantly, while the acceleration voltage had no significant influence. Furthermore, an extended collector distance led to slightly thinner fibers. In addition to that, the different spinneret diameters gave information about the necessity of mass flow balancing between the feeding system and the electrohydrodynamic fiber drawing process to minimize their dynamic swaying and the occurring pulsing failures. In general, it is key to use the appropriately sized spinneret for the polymer melt of interest, to prevent the dynamic fluctuation of the jet. Working with sufficiently small spinneret is required in order to electrospin homogeneous and well-designed fiber structures from melts.

Acknowledgments

This work was financially supported by the European research council (ERC consolidator grant Design2Heal, contract no° 617989). We thank Prof. Würthner and Dr. Stepanenko for the possibility of SEM measurements within the Wilhelm Conrad Röntgen Research Center Würzburg.

Appendix A. Supplementary data

Supplementary data related to this article can be found at http://dx.doi.org/10.1016/j.polymer.2014.08.024.

References

[1] Hoogenboom R, Thijs HML, Jochems MJHC, van Lankvelt BM, Fijten MWM, Schubert US. Chem Commun 2008;44:5758. http://xlink.rsc.org/?DOI=b813140f.

[2] Luxenhofer R, Jordan R. Macromolecules 2006;39(10):3509. http://dx.doi.org/3510.1021/ma052515m.
[3] Hoogenboom R. Angew Chem Int Ed 2009;48(43):7978. http://onlinelibrary.wiley.com/doi/7910.1002/anie.200901607/abstract.
[4] Schlaad H, Diehl C, Gress A, Meyer M, Demirel AL, Nur Y, et al. Macromol Rapid Commun 2010;31(6):511. http://onlinelibrary.wiley.com/doi/2010.1002/marc.200900683/abstract.
[5] Tacey X, Viegas MDB. Bioconjugate Chem 2011;22(5):976.
[6] Hartlieb M, Pretzel D, Englert C, Hentschel M, Kempe K, Gottschaldt M, et al. Biomacromolecules 2014;15(6):1970.
[7] Dworak A, Utrata-Wesołek A, Oleszko N, Wałach W, Trzebicka B, Anioł J, et al. J Mater Sci Mater Med 2014;25(4):1149. http://link.springer.com/article/1110.1007/s10856-10013-15135-10857.
[8] Bloksma MM, Paulus RM, van Kuringen HPC, van der Woerdt F, Lambermont-Thijs HML, Schubert US, et al. Macromol Rapid Commun 2012;33(1):92. http://onlinelibrary.wiley.com/doi/2010.1002/marc.201100587/abstract.
[9] Christova D, Velichkova R, Loos W, Goethals EJ, Prez FD. Polymer 2003;44(8):2255. http://www.sciencedirect.com/science/article/pii/S0032386103001393.
[10] Gaertner FC, Luxenhofer R, Blechert B, Jordan R, Essler M. J Control Release 2007;119(3):291. http://www.sciencedirect.com/science/article/pii/S0168365907001174.
[11] Goddard P, Hutchinson LE, Brown J, Brookman LJ. J Control Release 1989;10(1):5. http://www.sciencedirect.com/science/article/pii/0168365989900138.
[12] Adams N, Schubert US. Adv Drug Deliv Rev 2007;59(15):1504. http://www.sciencedirect.com/science/article/pii/S0169409X07001901.
[13] Brown TD, Dalton PD, Hutmacher DW. Adv Mater 2011;23(47):5651.
[14] Brown TD, Slotosch A, Thibaudeau L, Taubenberger A, Loessner D, Vaquette C, et al. Biointerphases 2012;7(1–4):13.
[15] Farrugia BL, Brown TD, Upton Z, Hutmacher DW, Dalton PD, Dargaville TR. Biofabrication 2013;5(2):025001. http://iopscience.iop.org/021758-025090/025005/025002/025001.
[16] Dalton PD, Vaquette C, Farrugia BL, Dargaville TR, Brown TD, Hutmacher DW. Biomaterials Sci 2013;1(2):171. http://xlink.rsc.org/?DOI=c172bm00039c.
[17] Srinivasan G, Reneker DH. Polym Int 1995;36(2):195.
[18] Pham QP, Sharma U, Mikos AG. Tissue Eng 2006;12(5):1197.
[19] Bhardwaj N, Kundu SC. Biotechnol Adv 2010;28(3):325.
[20] Hutmacher DW, Dalton PD. Chemistry-An Asian J 2011;6(1):44.
[21] Pfitzner J. Anaesthesia 1976;31(2):273. http://onlinelibrary.wiley.com/doi/210.1111/j.1365-2044.1976.tb11804.x/abstract.
[22] Sutera SP, Skalak R. Annu Rev Fluid Mech 1993;25(1):1. http://www.annualreviews.org/doi/pdf/10.1146/annurev.fl.1125.010193.000245.
[23] Wei C, Dong J. J Micromechanics Microengineering 2013;23(2):025017. http://stacks.iop.org/020960-021317/025023/i=025012/a=025017?key=crossref.025013ca025011c025032S100d025013dcfe025015c025549ef095372f025021c025048.
[24] Zhmayev E, Zhou H, Joo YL. J Newt Fluid Mech 2008;153(2–3):95.